

## Research Article

Tao Meng\*, Jiaolong Zhang, Huadong Wei, and Jiajia Shen

# Effect of nano-strengthening on the properties and microstructure of recycled concrete

<https://doi.org/10.1515/ntrev-2020-0008>

Received Sep 23, 2019; accepted Oct 15, 2019

**Abstract:** Influence of nano-strengthening immersion on the properties of recycled aggregate (RA) and recycled aggregate concrete (RAC) and the microstructure of interfacial transition zones (ITZs) between mortar and aggregate were studied in this paper. Results showed that nano-strengthening immersion was helpful to reduce the crushing value and total pore area of RA, to significantly improve the mechanical strength of RAC, and to modify the bond strength between RAC and steel rebar and the structural properties of RAC beams. Mercury intrusion porosimetry (MIP), micro-hardness (MH) and scanning electron microscope (SEM) observation were conducted in order to reveal the enhancement mechanism of nano-strengthening immersion. Results showed that the density and mechanical properties in ITZs were obviously improved by nano-strengthening because the coating and penetration of nano-materials was helpful to block the pores and cracks in ITZs, to avoid the directed gathering of CH crystal, and to accelerate the hydration of cement and mineral additions.

**Keywords:** nano-strengthening, mechanical properties, recycled concrete, recycled aggregate, interfacial transition zones

## List of Abbreviations

**C&DW** construction and demolition wastes  
**EMV** mortar volume method  
**ITZs** interfacial transition zones  
**MH** micro-hardness  
**MIP** mercury intrusion porosimetry  
**NA** natural aggregate  
**NAC** natural aggregate concrete  
**RA** recycled aggregate  
**RAC** recycled aggregate concrete  
**SEM** scanning electron microscope  
**TSMA** two-stage mixing approach

## 1 Introduction

Concrete is the most widely used building material in construction industry. Nowadays, it is estimated that the production of concrete may achieve more than 6 billion tons per year in the world. This causes severe environmental problems including the increasing shortage of natural aggregates and the pollution on the process of concrete production. The valuable utilization of construction and demolition wastes (C&DW) may well be the reasonable and prospective way to deal with those problems [1].

The reuse of C&DW have been conducted for more than thirty years in order to reduce the amount of C&DW disposed of in landfilling and to preserve natural resources. It is reported that the recycling level in Holland and Belgium reached almost 90% in the late of 1990s while it was still less than 50% in many other developed countries [2–4]. Nowadays, the problems from C&DW are increasing up because of the accelerating urbanization in the developing countries, especially in China, Brazil and India [5–7]. Although the recycling for C&DW has been conducted for more than 50 years, but till now it only covers the use of coarse aggregates and their use is restricted due to the low strength and elastic modulus, bad workability, high water infiltration, high shrinkage and creep of RAC [8, 9].

**\*Corresponding Author: Tao Meng:** College of Civil Engineering and Architecture, Zhejiang University, Hangzhou, 310058, China; Email: taomeng@zju.edu.cn

**Jiaolong Zhang:** College of Civil Engineering and Architecture, Zhejiang University, Hangzhou, 310058, China; College of civil engineering, Tongji University, Shanghai, 200092, China

**Huadong Wei:** College of Civil Engineering and Architecture, Zhejiang University, Hangzhou, 310058, China

**Jiajia Shen:** College of Civil Engineering and Architecture, Zhejiang University, Hangzhou, 310058, China; Bristol Composite Institute (ACCIS), University of Bristol, Bristol, BS8 1TR, United Kingdom of Great Britain and Northern Ireland

Due to the low density and high porosity of RA, RAC may well be significantly more permeable than natural aggregate concrete (NAC) [10, 11], and the compressive strength of RAC could probably be much less than that of NAC [12, 13]. Moreover, RA also performed a harmful influence on durability of RAC due to the presence of weak and porous particles in RA and the low concentration of original coarse aggregate in RAC, especially the resistance of freezing and thawing [14–17]. And the maximum replacement of natural aggregate (NA) by RA was still restricted to less than 50% in many countries in order to ensure the properties of concrete [18, 19]. The structural properties of RAC were started to study after 2000s in order to apply RAC into actual engineering [20]. It is shown that the ultimate strain of RAC decreased with the increase of the replacement by RA from the results of axial compression test [20], and the tensile and bond strength of RAC beams also decreased from 9.4% to 21.3% [21]. Although the replacement of 50% coarse NA by RA showed a slight effect on the deflections and the ultimate loads from the shear test results of RAC beams [22], however, the creep and shrinkage of RAC with 100% RA increased 51% and 70%, respectively [23]. Moreover, it is believed that the main reason for the low Young's modulus, high peak strain and high brittleness of RAC was the large volume content of new and old hardened mortar in RAC, especially the large amount of weak old mortar in RA [24, 25]. It can be concluded that RA performed a severe negative influence on the properties of concrete due to the high water absorbability, the weak interfacial ITZs and the high content of mortar.

In recent years, many attempts have been conducted in order to improve the fluidity, mechanical properties and durability of RAC through many technical methods including the modification of mixing process, the pre-wetting or surface-coating for RA, and the modification of physical properties of RA and cohesive force in ITZ by adding mineral admixtures, superplasticizer, polymer, fibers.

Modification of mixing process showed a positive influence on the properties of RAC. A new mixing method named two-stage mixing approach (TSMA) was proposed and showed a significant enhancement for compressive strength of RAC, especially for that at early ages and with high replacement ratio by RA. Moreover, it seemed that cracks in RA could probably be filled after adopting TSMA [26, 27]. Compared to air-dried and oven-dried RAs, saturated surface-dried RA probably imposed the largest negative effect on compressive strength of RAC due to the “bleeding” of excess water in fresh concrete even if it provided the maximum fluidity of fresh concrete [28]. Moreover, a new triple mixing method developed from TSMA and surface-coating showed a further improvement for the

compressive strength and the Coulomb charge passed in RAC [29–31]. In view of the high amount of cement mortar in RAC, a new equivalent mortar volume method (EMV) which regarded the total mortar volume as the sum of residual and fresh mortar volume in RAC was developed for the mix design method of RAC. Experimental results indicated EMV method could increase the density of fresh and hardened RAC, and improve the mechanical and structural properties in RAC structures [32].

Some specific materials were adopted to modify the properties of RAC. It was said that fly ash and silica fume with extra superplasticizer could improve the fluidity and mechanical properties of RAC with 100% RA and the ultimate load of RAC beams [33]. The similar result was reported in the research of rice husk-bark ash which was a main agricultural by-product in Thailand [34]. Moreover, polypropylene fibers and metallic fibers were helpful to reduce the width of crack and free shrinkage of RAC [35]. At the same time, microwave-assisted technique was even used to enhance the quality of RA [36]. Thermal treatment was also used to achieve the rehydration of cement mortar in RA and enhance the properties of RAC [37]. Results implied the dehydration and transformed components, which was formed from the initial cement products when the temperature increased up to 500°C, could rehydrate and significantly increase the compressive strength of cement mortar in RA.

Because the strength of adhered mortar in RA usually was much lower than that in NA and new cement paste, therefore the porous ITZ which may probably be the weakest point in RAC could obviously affect the properties of RA and RAC [38, 39]. A Modeled Recycled Concrete was studied by nanoindentation tests and results showed that ITZs had a significant effect on stress-strain response and failure patterns [40]. Thus, how to strengthen the ITZs and old cement mortar have become the key point for the development of high strength RAC and the wide application of RAC in construction engineering.

Some valuable progresses have obtained in this area by adding the cementitious materials in recent years, however, most of them only focused on the ITZ between the NA and new cement mortar while other two types of ITZs, between NA and old mortar, and between old mortar and new mortar, seemed to be ignored [24]. Moreover, it is difficult to modify the ITZ between NA and old mortar which is generally the weakest zone in RAC due to the limited permeability of these cementitious materials. Therefore, if a specific material can penetrate into the RA and reduce the porosity of this ITZ, it will be very helpful to improve the mechanical properties and durability of RAC. At present, the influence of nano-materials on the properties of con-

crete has been concentrated widely due to the significant improvement in mechanical strength and durability of concrete. It was said that nano-SiO<sub>2</sub> could improve the density of concrete even under the same fluidity of concrete [41], and nano-SiO<sub>2</sub> and nano-TiO<sub>2</sub> were helpful to refine the pore structure and enhance the resistance of chloride penetration of concrete [42, 43]. Moreover, the formation of C-S-H gel could also be accelerated by these nano-materials especially at the early ages and the nano-filling was much helpful to decrease the amount of harmful pores in concrete [44–46].

Nano-strengthening for RA was studied by nanoindentation and three beams in a real building including nano-silica modified recycled aggregate beam was tested [47, 48]. Results proved that nano-strengthening may well be a suitable modification method for RAC although the relative research on the effect of nano-strengthening on the properties and microstructure of RA and RAC hasn't published. In this paper, nano-SiO<sub>2</sub> gel and nano-CaCO<sub>3</sub> slurry were expected to perform as the available nano-strengthening immersion solutions for the modification of RA due to their high activity and high penetrability through the mechanical and structural experiments of RA and RAC. Meanwhile, the enhancement mechanism of nano-strengthening for RAs and ITZs in RACs was also attempted to reveal by Mercury Intrusion Porosimetry (MIP) analysis, Micro-hardness (MH) tests and Scanning Electron Microscopy (SEM) observations.

## 2 Materials and experiment

### 2.1 Materials

#### Cement

Commercial P.O42.5R type of Portland cement according to Chinese National Standard GB 175-2007 produced by Lafarge Cement Company, China was used for this experiment.

#### Recycled coarse aggregate

RA with size fraction from 4.75mm to 19.0mm, which was broken by the jaw crusher from the abandoned concrete in concrete companies with the original compressive strength approximately from 20MPa to 40MPa, was used in this experiment.

#### Fine aggregate

Commercial mixed sand with fineness modulus of 2.5, which was widely used in China for the construction, produced in Zhejiang by mixing high fine sand and artificial sand which was broken from the coarse gravel with the proportion of 80% and 20% respectively was used for this experiment.

#### Superplasticizer

A naphthalene-based superplasticizer with 25% water reduce ratio produced by Wulong Company of Zhejiang was selected for this experiment.

#### Fly ash

Commercial Grade-II type of fly ash according to Chinese National Standard GB/T 1596-2005 produced in Changxing Power Plant, Zhejiang was adopted in this experiment.

#### Nano-CaCO<sub>3</sub> slurry

Nano-CaCO<sub>3</sub> slurry produced in Institute of Building Materials in Zhejiang University, with the solid content of 12% and size fraction from 30nm to 50nm was considered in this experiment.

#### Nano-silica sol

Commercial GS-30 type of Nano-silica sol produced by Zhejiang Yuda Chemical Co., Ltd., with the solid content of 30.5%, PH value of 10.4, viscosity of 6.9cP and particle size fraction from 8nm to 20nm was used in this experiment.

#### Steel rebar

low-carbon steel rebar with the yield strength of 235MPa, the ultimate tensile strength of 370MPa and the nominal diameter of 10mm was used in this experiment.

## 2.2 Experimental methods of RA

### Immersion strengthening method

Nano- $\text{CaCO}_3$  slurry and nano- $\text{SiO}_2$  sol were chosen to perform as the strengthening solution. After mixed these materials with tap water according to the mix proportions shown in Table 1, RAs were immersed into the different nano-strengthening solutions and removed after 45min immersion. Then the strengthened RAs were dried at  $20 \pm 2^\circ\text{C}$  and RH of  $65 \pm 5\%$  for at least 3 days in order to test the related properties, or removed to drain in order to achieve the saturated surface-dried condition for mixing.

**Table 1:** Proportion of the Immersion solutions (%)

Specimen number	Nano- $\text{CaCO}_3$ slurry	Nano- $\text{SiO}_2$ sol	Water
A0	/	/	100
A1	5	/	95
A2	/	5	95
A3	5	5	90

*Note: The content of nano-materials represented the real solid content, not the dosage of nano-material solutions.*

### Crushing value

Approximate 3kg weight of RAs with the particle diameter between 9.5 mm and 19.0mm were placed into the steel cylinder. After vibrating the cylinder with a round steel bar for 25 times in order to compact the RAs according to Chinese national standard GB/T 14685-2011, the RAs were loaded with the speed of approximate 1kN/s to the ultimate load of 200 kN and then slowly unloaded five seconds later. Thus the weight of crushed aggregates could be weighed and the crushing value could be calculated after sieved the crushed aggregates with the diameter below 2.36 mm.

### Water absorption ratio

After the RAs were immersed under the water for  $24 \pm 0.5\text{h}$ , the water on the surface of RAs was removed by a wet towel and the weight of RAs in the saturated surface-dried condition was measured. After that, the RAs were placed into the oven and dried at  $105 \pm 5^\circ\text{C}$  for  $24 \pm 0.5\text{h}$  in order to obtain the weight of RAs in the oven-dried condition. Thus, the water absorption ratio could be calculated

according to Chinese national standard GB/T 14685-2011. Table 2 showed the experimental results of crushing value and water absorption ratio of RAs.

### Mercury intrusion porosimetry (MIP) analysis

The RAs with the particle diameter between 2.5mm to 5mm were chosen and conducted the mercury penetration experiment by Micromeritics AutoPore IV 9500 Series Pore Size Analyzer from Zhejiang University Polymerization and Polymer Engineering Laboratory. Then the results were analyzed by porosity analysis software and total pore area in RAs which was shown in Table 2 could be obtained.

**Table 2:** Physical properties and total pore area of RAs with or without strengthening

Specimen number	Crushing value (%)	Water absorption ratio (%)	Total pore area ( $\text{m}^2/\text{g}$ )
A0	15	8.45	15.579
A1	11.6	8.38	11.309
A2	10.9	9.68	8.962
A3	12.7	6.88	6.915

### Scanning electron microscope (SEM) observations in RAs

The RAs were crushed and the particles with the diameter less than 1cm were selected to conduct the SEM test. After those small particles were sprayed with gold for 60s in SBC-12 Small Particles Sputtering Apparatus to make them conductive, the microscopic structures of those specimens under different magnifications were observed with TM3000. Figures 1 and 2 showed the micro-morphology of ITZs in specimen A0 and A3, respectively.

## 2.3 Experimental methods of RAC

### Mix proportion

In order to study the effect of nano-strengthened RAs on the mechanical properties, structural properties and the microstructure in ITZs of RACs, the RACs with the similar fluidity were mixed according to the mix proportion shown in Table 3 The reference concrete was mixed by the original

**Table 3:** Mix proportions and physical properties of recycled concrete

Specimen number	Cement	Mix proportions of concrete (kg/m <sup>3</sup> )			RAs	slump (mm)	apparent density (kg/m <sup>3</sup> )	Strengthening solution
		Water	Superplasticizer	Sand				
A	307	197	5.4	785	1000	160	2320	/
B	307	197	5.4	785	1000	160	2320	5% Nano-CaCO <sub>3</sub> Slurry + 5% Nano-SiO <sub>2</sub> Sol
C	358	229	6.2	763	970	200	2290	5% Nano-CaCO <sub>3</sub> Slurry + 5% Nano-SiO <sub>2</sub> Sol
D	365	233	6.1	756	962	150	2290	5% Nano-CaCO <sub>3</sub> Slurry + 1% Dispersant

Note:

1. The percentages in strengthening solutions represented the real solid content of nano-materials.

2. The dosage of superplasticizer was recommended by the producer and adjusted according to the similar slump of concrete.

The water absorbed by the RAs was not including in the dosage of water.

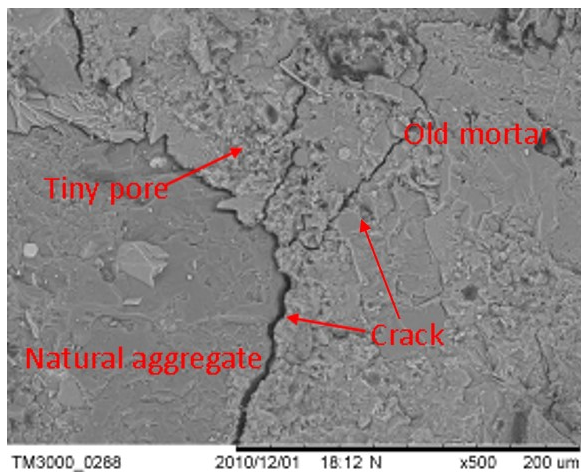


**Figure 1:** Micro-morphology of ITZ in recycled aggregate of Specimen A0

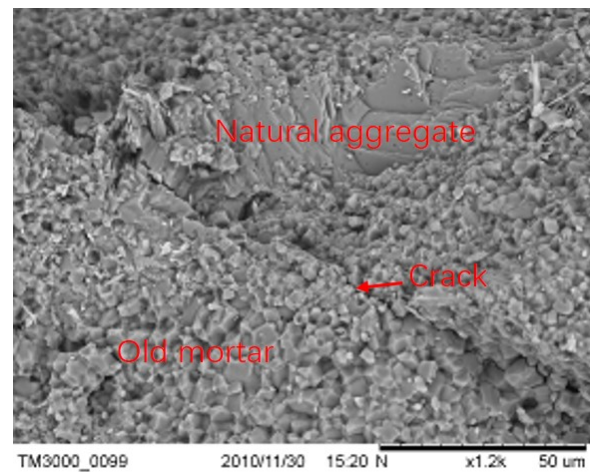


**Figure 2:** Micro-morphology of ITZ in recycled aggregate of Specimen A3

RAs and the other three concretes were produced by the strengthened RAs. In addition, the target strength grade of reference concrete was designed as C25 with the water-binder ratio of 0.59, the over-replacement index of fly ash was 1.5 and the volume fraction of sand to total aggregate was 44%. In view of the significant effect of combined nano-solutions on the physical properties and pore distribution of RAs, A3 was determined to perform as the major nano-strengthening solution of RAs. Meanwhile, in order to modify the dispersion of nano-materials in the nano-strengthening process of RAs, nano-CaCO<sub>3</sub> slurry with dispersant was considered as another nano-strengthening solution. Moreover, the content of cement paste with the same water-binder ratio varied slightly in order to achieve the similar slump because of the effect of different RAs on

the fluidity of concrete. Table 3 showed the mix proportion and nano-strengthening solution of RACs.

### Mixing procedure

As for the mixing procedure, a revised method from the two-stage mixing approach (TSMA) and the surface-coating mixing procedure was adopted in this experiment in order to satisfy the requirement of nano-strengthening and mixing process. Figure 3 illustrated the flow process chart of this mixing procedure. After immersing into the nano-strengthening solutions or tap water for 45 min, the RAs were removed to drain in order to achieve the saturated surface-dried condition. Then the RAs were mixed with half of the cementitious materials for 30s, and later



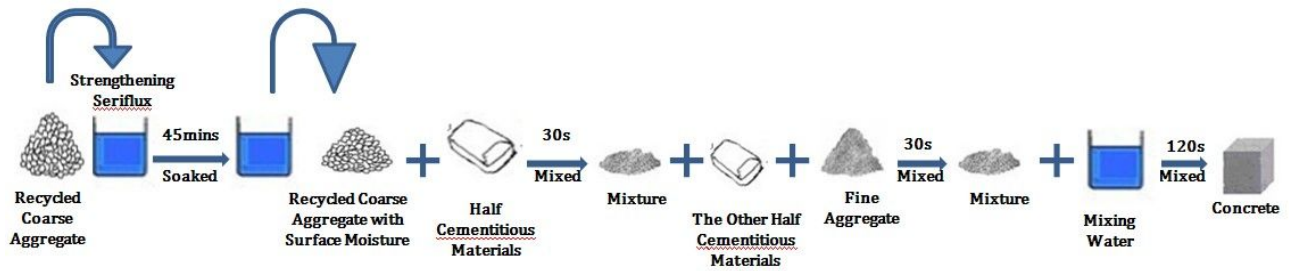


Figure 3: Mixing procedure of recycled aggregate concrete (RACs)

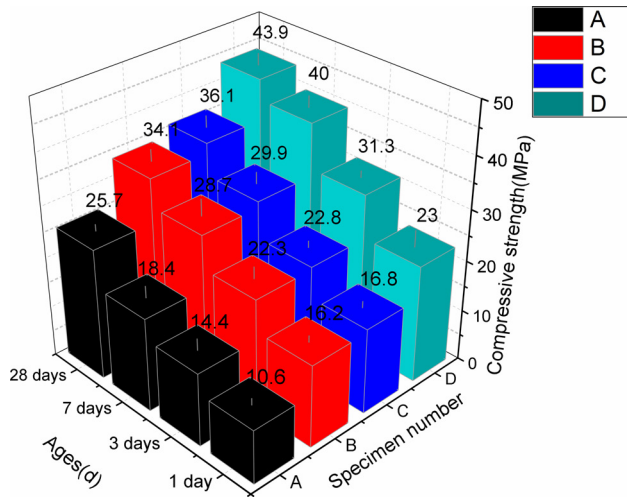


Figure 4: Compressive strength of RACs at different ages

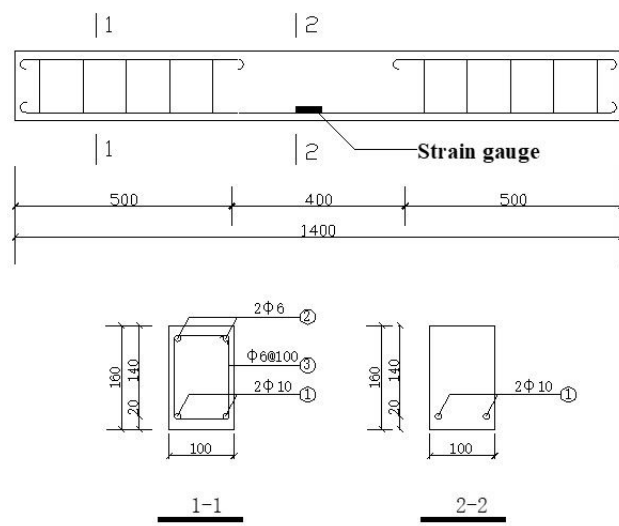


Figure 5: Design details of the beam

mixed with fine aggregates and another half of cementitious materials for another 30s. Finally, the mixing water was added into and mixed for 120s. Thus the fresh RACs after nano-strengthening and mixing were produced and casted to perform the experiments.

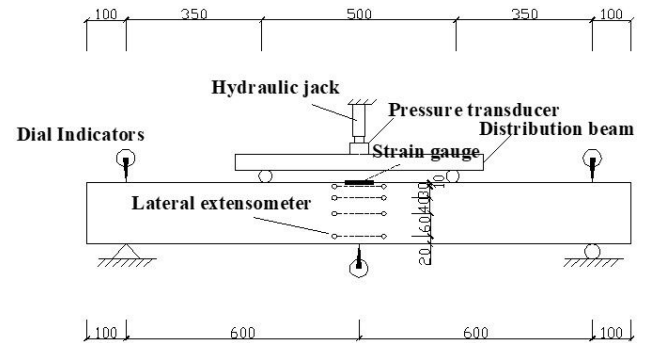


Figure 6: Experimental arrangement of stress and strain equipment in beam test

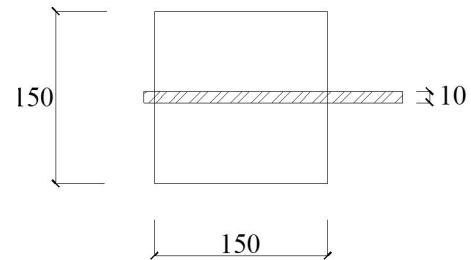


Figure 7: Schematic illustration of the central pullout test

### Compressive strength test

After demoulded at 1 day, RACs were conserved into the water at  $20 \pm 2^\circ \text{C}$  and the compressive strength was conducted at specific ages according to Chinese national standard GB/T 50081-2002. Figure 4 showed the compressive strength of RACs at different ages.

### Beam test

In order to understand further information about the effect of nano-strengthening immersion on the structural properties of RACs, four beams were casted according to the four different mix proportions of RACs. Meanwhile, in order to remove the shearing force, a kind of distribution beam to

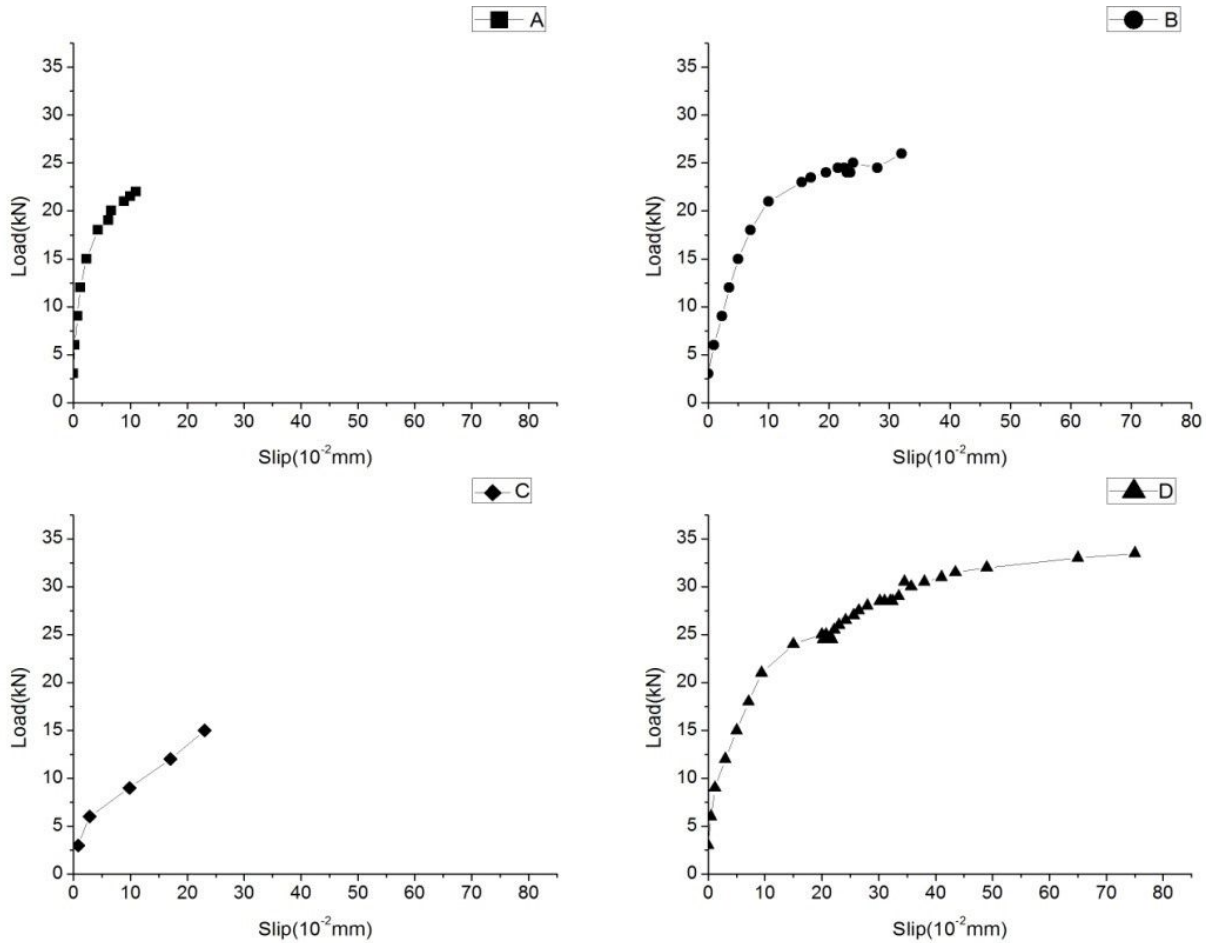


Figure 8: Load-slip curves of pullout test

form a pure bending section with a length of 500mm at the mid span was designed. The strain of concrete and steel rebar, the deflection and the load of those beams had been measured according to Chinese Standard for test method of concrete structures GB/T 50152-2012. Figures 5 and 6 indicated the design details of these beams including the reinforcement condition and the experimental arrangement of stress and strain equipment in beam test, respectively.

### Pullout test

The schematic illustration of the central pullout test was shown in Figure 7 according to the Chinese Standard “Test code for hydraulic concrete” (DL/T 5150-2001). The load and the slip at the free end of steel rebar anchored in the RAC specimens were measured artificially in order to obtain the relationship between load and slip in different specimens. Figures 7 and 8 showed the schematic illustration

and experimental results of central pullout test, respectively.

### Micro-hardness (MH) test method in ITZs

Concrete at certain curing age was cut to several slices with the depth of 5mm. Vickers micro-hardness value in ITZs was measured at each 30  $\mu$ m distance from the interface between the aggregate and mortar by DHV-1000 Digital Microscopic Vickers Hardness Tester. Figure 9 showed the difference between specimen A and specimen D of micro-hardness in different ITZs.

### SEM observations in RACs

The RACs were molded and conserved in the water at  $20 \pm 2^\circ \text{C}$ . Then the RACs at certain curing age were broken into small fragments and the hydration of cement was

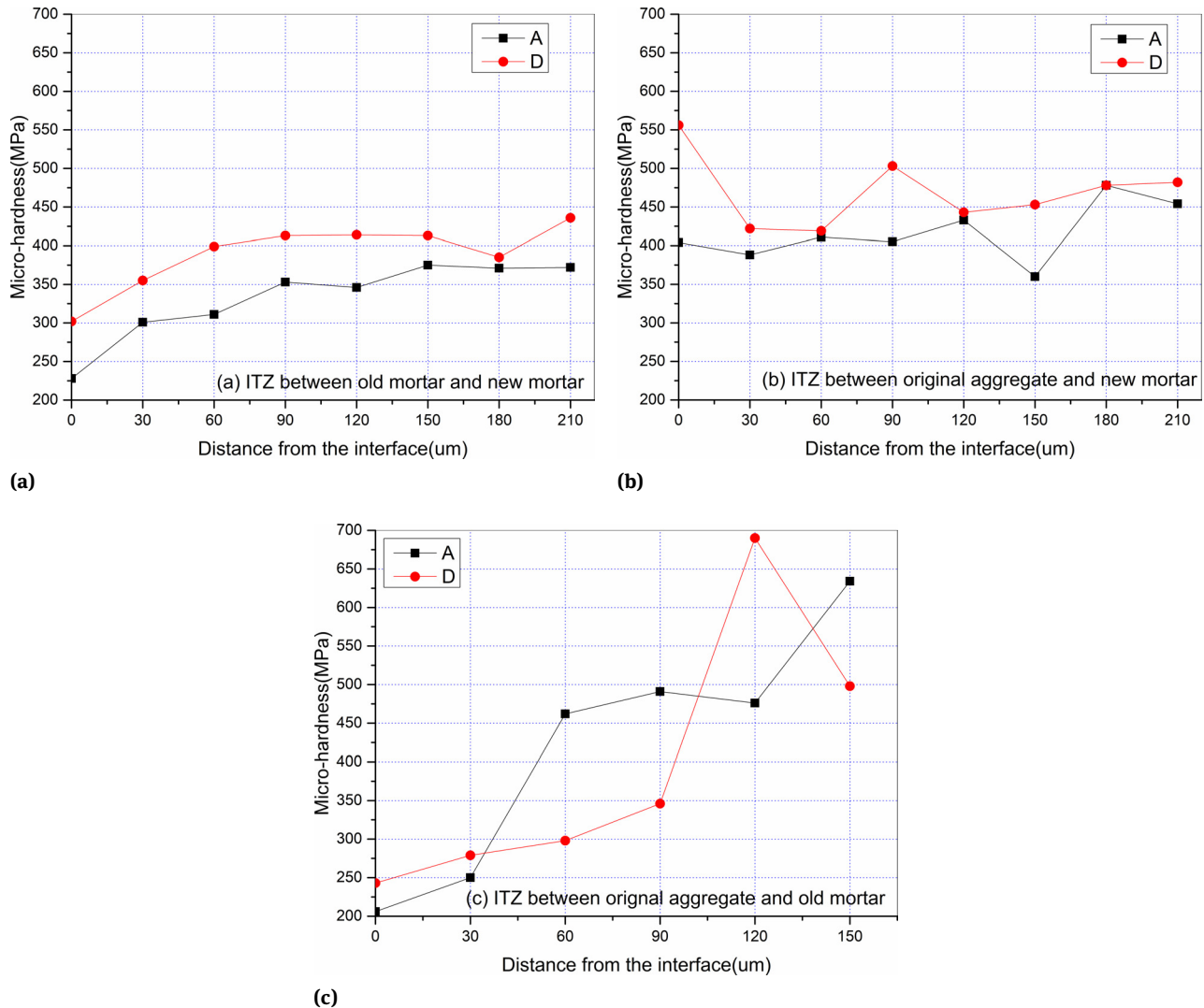


**Figure 9:** Micro-hardness in different ITZs of specimen A and specimen D a) ITZ between old mortar and new mortar; b) ITZ between original aggregate and new mortar; c) ITZ between original aggregate and new mortar

stopped by pure alcohol at specific age. In order to distinguish the different kinds of ITZs, the appearance of those small fragments was sketched before they were sprayed with gold for 60s in SBC-12 Small Particles Sputtering Apparatus to make them conductive. Microscopic structures in different ITZs of specimens under different magnifications were observed with TM3000. Figures 10 to 12 presented the SEM images in three different ITZs of specimen A and specimen D, respectively.

## 3 Results and discussion

### 3.1 Results and discussion of RA experiment

Table 1 showed the mix proportion of nano-strengthening solutions. In order to study the efficacy of nano-materials on the properties of RA, specimen A was immersed into the water as the reference RA while other specimens were placed under the nano-strengthening solutions. Table 2 indicated the change of properties in RAs with or without nano-strengthening. Results showed nano- $\text{CaCO}_3$  slurry and nano-silica sol could reduce the crushing value for approximately 23% and 27%, respectively. It was helpful to increase the mechanical properties of RAC. However, the re-



sults of water absorption experiment were depressed due to the extra high water absorbability of nano-materials on the surface of RAs. Moreover, the water absorption ratio of specimen A2 was a little higher than that of reference specimen because nano-silica sol could form a thin film on the surface of RAs and prevent the water in RAs from evaporation. It is pointed out that the different test methods of water absorption would cause the different results and a new approach named real-time assessment of water absorption is presented [49]. Therefore, the traditional water absorption test may not achieve a satisfied accuracy of results for these nano-strengthened RAs. Further research will be designed and tested in order to find the proper method for the test of water absorption.

Table 2 also showed the difference of pore distribution in RAs with and without nano-strengthening. Compared to specimen A0, the total pore area of other three specimens were much lower due to the significant influence of nano-strengthening. After strengthened by nano- $\text{CaCO}_3$  slurry and nano-silica sol solutions, the total pore area of specimens decreased approximately 27.5% and 42.5%, respectively. Moreover, combined nano-solutions showed the best influence and reduced 55.6% total pore area.

Figures 1 and 2 indicated the micro-morphology images of ITZ between original aggregate and old mortar in specimen A0 and A3, respectively. Compared to specimen A3, many cracks and tiny holes could be found in specimen A0 due to the original loosen ITZ in parent concrete and the damage on the manufacture process of RA. After strengthened by combined nano-solutions, many tiny crystals were settling on the surface of RA and blocking the cracks in ITZ and RA. Therefore, the density in ITZ of specimen A3 was improved and the cracks became hazy and discontinuous.

It can be concluded that combined nano-solutions presented a significant influence on the physical properties and microstructure of RAs from these experimental results. Thus, the experiments of RAC with 100% RAs nano-strengthened by the combined nano-solutions were conducted in order to reveal the effect of nano-strengthening on the mechanical properties of RACs and microstructure in ITZs and achieve the available performance of RA for the high strength and strong durability concrete.

### 3.2 Results and discussion of RAC experiments

According to the target strength grade of C25, the water-binder ratio was calculated as 0.59 while the over-replacement index of fly ash and the volume fraction of sand to total aggregate were determined as 1.5 and 44%, re-

spectively. At the same time, two strengthening solutions were selected. One was combined nano-solution with 5% nano- $\text{CaCO}_3$  slurry and 5% nano- $\text{SiO}_2$  sol, the other was the solution with 5% nano- $\text{CaCO}_3$  slurry and 1% dispersant for improving the dispersivity of nano-materials in concrete and reducing the cost of nano-strengthening. Moreover, two mix proportions with the extra dosage of cement paste were designed in order to maintain the similar fluidity of specimen A and specimen D, and compare the different influence between these two nano-solutions. Table 3 showed the mix proportion and physical properties of RACs.

In addition, a revised method from the two-stage mixing approach and the surface-coating mixing procedure was adopted in this experiment in order to exhibit the efficiency of nano-strengthening. Figure 3 illustrated the mixing procedure of RACs.

Figure 4 showed the compressive strength of RACs at different ages. Considering to the target design strength of 25MPa, the compressive strength of RAC with 100% RA at 28 days was 25.7MPa, a little lower than the calculation target strength from Chinese professional standard JGJ 55-2011 of common concrete with 100% natural aggregate due to the high porosity and high-water absorption of RA. However, the compressive strength of specimen B strengthened by combined nano-solution at 1 day, 3 days, 7days and 28 days were much higher than that of specimen A without strengthening for approximately 52.8%, 54.9%, 56.0%, 32.7%, respectively. Compared to specimen B, the compressive strength of specimen C only increased less than 10%. This meant nano-strengthening could provide more effective improvement on mechanical strength than the amount increase of cement paste with the same cement-binder ratio. As for the two nano-solutions, 5% nano- $\text{CaCO}_3$  slurry with 1% dispersant indicated a better influence because the compressive strength of specimen D at 1 day, 3 days, 7days and 28 days were higher than that of specimen C for approximately 36.9%, 37.3%, 33.8%, 21.6%, respectively. The possible reasons were the adhesion force between the RA and new mortar could be reduced by the film formed by nano-silica sol and the dispersivity of nano-materials may be enhanced by dispersant.

Figures 5 and 6 showed the design details and the experimental arrangement in beam test, respectively. Table 4 indicated the experimental results including the force and moment of RAC beams. Results implied the influence of nano-strengthening was different between the compressive strength test and the beam test. Compared to the specimen A, the ultimate force and ultimate moment of specimen D only increased approximately 5.7% and 6.4%, respectively. Moreover, the force and moment of specimen C

**Table 4:** Experimental results of beam test at 28 days

Specimen number	Force(kN)		Moment(kN·m)	
	Yielding Force	Ultimate Force	Yielding Moment	Ultimate Moment
A	39	48.4	6.83	8.47
B	40	49.7	7.01	8.7
C	38.3	43.3	6.71	7.58
D	42.3	51.5	7.42	9.01

showed an unexpected decrease. Consequently, the study on the behavior of strengthened RAC under different load and environment should be paid more close attention in the future.

Figures 7 and 8 presented the schematic illustration and the load-slip curves of the central pullout test. Because the cohesive stress along the whole anchorage length of the steel rebar had been considered as uniform distribution, bond strength could be worked out by the equation (1):

$$\tau_0 = P_u / \pi d l_a \quad (1)$$

$\tau_0$  – bond strength (MPa)

$P_u$  – ultimate force (N)

$d$  – diameter of steel rebar (mm)  $l_a$  – anchorage length (mm)

It seemed that the ultimate forces and bond strength of specimen B and D were higher than that of specimen A for approximately 25.0% and 44.2%, respectively. This indicated 5% nano- $\text{CaCO}_3$  slurry with 1% dispersant could significantly improve the bond strength between RAC and steel rebar. Moreover, the slip of specimen B and D were also enlarged. Even if the data of specimen C decreased slightly, it still can be concluded that nano-strengthening was helpful to enhance the mechanical properties in pull-out test.

Combined nano-solutions and 5% nano- $\text{CaCO}_3$  slurry with 1% dispersant represented a high ability for the strengthening of RAs from the compressive strength results, however, the results of beam test were not satisfied. This meant further research on the structural properties of RACs with nano-strengthening should be conducted in order to understand comprehensively the behavior under different loads and in different environment and achieve the requirement of engineering.

### 3.3 Results and discussion of microstructure experiment in ITZs of RAC

RAC could be regarded as a four-phase composite that included natural aggregates, old mortar, new mortar and interfacial transition zone (ITZ), and ITZ may probably be the weakest point in RAC [24]. Therefore, ITZ should be paid close attention because of the high porosity and close relationship with the mechanical properties and durability of concrete [50, 51].

In general the thickness of ITZ was typically 10  $\mu\text{m}$  to 50  $\mu\text{m}$ , it actually varied with many factors such as aggregate size, cement type and water-binder ratio [52]. Experimental results of pore size distribution, CH content and un-hydrated cement area test implied a more than 100  $\mu\text{m}$  thickness of ITZ in ordinary concrete [53–55]. In this study, the reference specimen A and specimen D strengthened by combined nano-solutions were selected to study the mechanism of nano-strengthening on the properties of RA and RAC. Meanwhile, micro-hardness (MH) test and SEM observations in three types of ITZs were adopted to investigate the change by nano-strengthening in ITZs which were regarded as a maximum 200  $\mu\text{m}$  area from the boundary to the bulk matrix.

Figure 9 showed the MH test results in three types of ITZs of specimen A and D at 3 days. Figure 9(a) indicated the MH value in ITZ between the old mortar and new mortar of specimen D was obviously higher than that of specimen A. The average MH value of specimen A and D were 332 MPa and 390 MPa respectively, which meant nano-strengthening was useful to increase the MH value in this ITZ. A similar result in ITZ between original aggregate and new mortar was presented in Figure 9(b). However, it seemed that the MH value in ITZ between original aggregate and old mortar of specimen A was similar with that of specimen D because the tiny particles of nano-solution was easy to cover the surface of RA but was still difficult to penetrate into the inner interface between original aggregate and old mortar.

Figures 10 to 12 indicated the micro-morphology images in different ITZs of specimen A and specimen D at

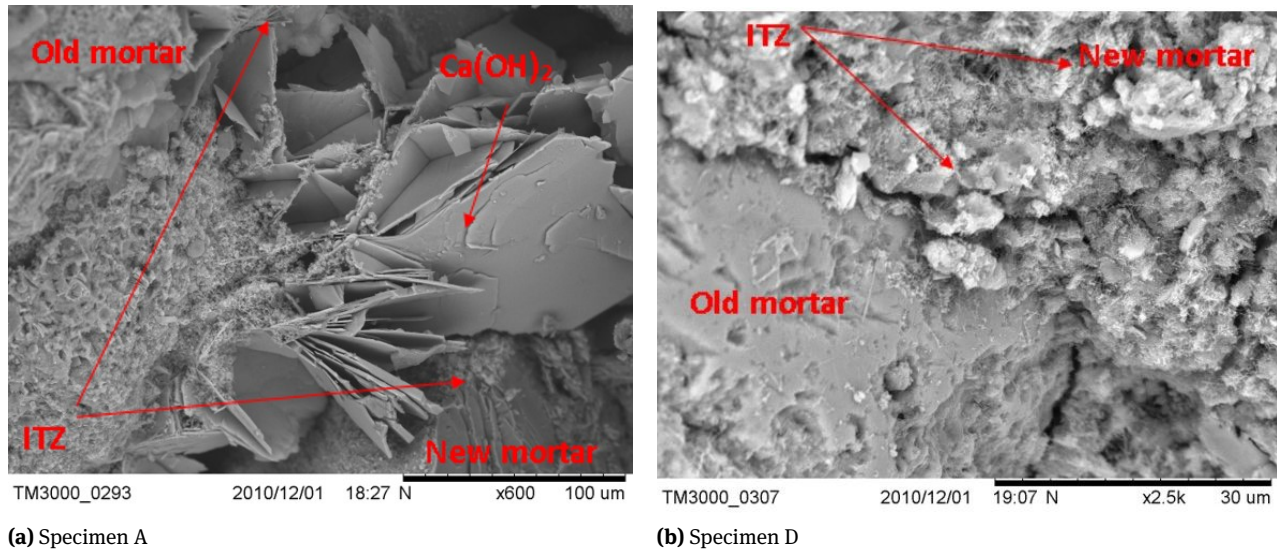


Figure 10: SEM images of ITZ between old mortar and new mortar in specimen A and D

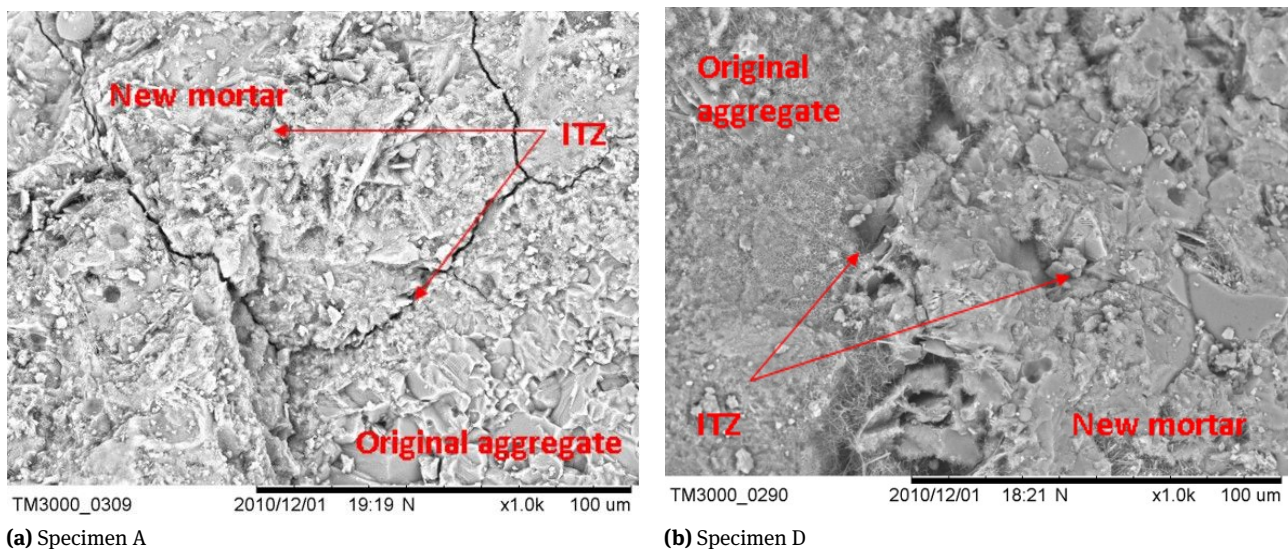
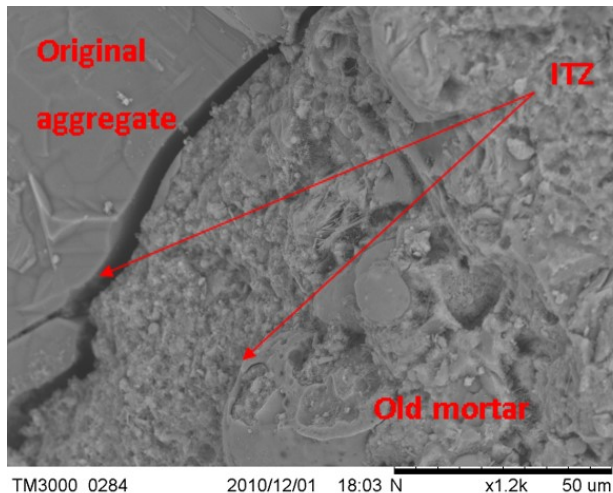


Figure 11: SEM images of ITZ between original aggregate and new mortar in specimen A and D

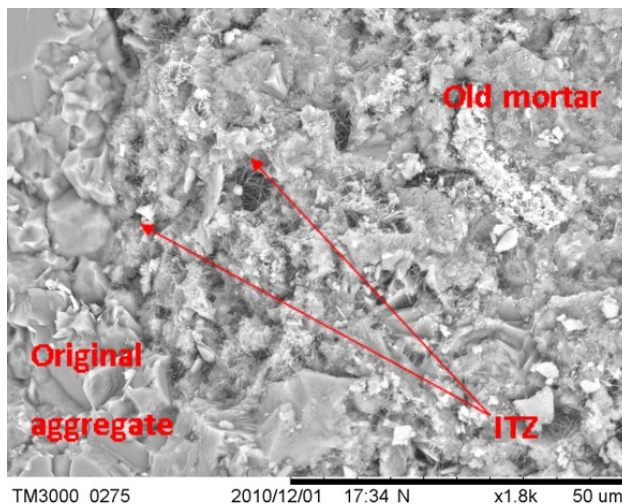
3 days. Figure 10(a) showed the SEM picture in ITZ between old mortar and new mortar of specimen A. The porosity was high and many codirectional large plate crystals which were CH could be found in the ITZ. This was very harmful to the mechanical properties and durability of concrete. However, it was different after nano-strengthening, which was shown in Figure 10(b). Many tiny crystals which might be formed by the reaction between nano-materials and cement minerals could be found in the ITZ. It was helpful to reduce the porosity and improve the mechanical properties. As for the ITZ between original aggregate and new mortar in specimen

A which was shown in Figure 11(a), there were many cracks due to the shrinkage and weak cohesion force. On the contrary, Figure 11(b) showed many tiny crystals formed in the boundary of aggregate and mortar after nano-strengthening and it was helpful to modify the cohesion force and block the crack and hole in ITZ. Figure 12 implied a potential influence of nano-strengthening on the ITZ between original aggregate and old mortar. Because of the long-time service and the damage on the manufacture process, the cracks were easy to create in the boundary of original aggregate and old mortar, which was very harmful to the properties of RA and RAC. Nano-materials could pen-





(a) Specimen A



(b) Specimen D

**Figure 12:** SEM images of ITZ between original aggregate and old mortar in specimen A and D

etrate into the cracks, fill and block them. Thus the porosity in ITZ could be improved and the cohesion force could be enhanced, which was very useful to the modification of mechanical properties and durability in RAC.

## 4 Conclusions

After revealed the effect of nano-strengthening of ITZs in RAC by nanoindentation and comparative research on the properties of nano-strengthening beams in a real building, the influence of nano-strengthening on the physical properties and pore distribution of RA and the mechanical and structural properties of RAC with 100% RA were continu-

ously studied in this paper. Meanwhile, the modifications in three ITZs by nano-strengthening were attempted to reveal through MH test and SEM observations.

It was verified that nano-strengthening immersion by the 5% nano- $\text{CaCO}_3$  slurry and 5% nano-silica sol could obviously reduce the crushing value of RA, however, it seemed to show a slight effect on water absorption because the water absorbability of nano-materials on the surface of RA might affect the accuracy of experimental results. Moreover, the combined nano-solutions mixed by 5% Nano- $\text{CaCO}_3$  slurry and 5% nano-silica sol revealed an more significant influence on the physical properties and pore distribution in RA than the one element nano-solution. After that, nano-strengthening was helpful to enhance the density of RA by nano-filling, surface-coating and hydration for nano-materials with cement minerals.

Experimental results indicated the obvious increase of compressive strength by nano-strengthening, not only at the beginning age but also at the late age. It was presented that compressive strength of RAC with 100% nano-strengthening RA at 1 day, 3 days, 7days and 28 days, which was mixed by a revised mixing procedure from two-stage mixing approach and surface-coating mixing procedure, increased 52.8%, 54.9%, 56.0%, 32.7%, respectively. Moreover, 5% Nano- $\text{CaCO}_3$  slurry with 1% dispersant showed higher strengthening efficacy than the combined nano-solutions. However, the results of RAC beam test and pullout test only provided a slight improvement of ultimate force, ultimate moment and bond strength, respectively. This also meant more structural experiments of nano-strengthening RAC need to conduct in order to understand comprehensively the structural behavior and achieve the similar satisfied efficacy as the compressive strength of RAC.

An approach on the nano-strengthening mechanism in ITZs was carried out by micro-hardness (MH) test and SEM observations. Results showed the density and mechanical properties in ITZs could be increased by nano-strengthening, because the coating and penetration of nano-materials could block the pores and cracks in ITZs, avoid the directed gathering of CH crystal and hydrate with cement minerals.

Nano-strengthening immersion indicated a valuable probability for the enhancement of RAs and the wide application of RACs in the actual engineering.

**Acknowledgement:** The authors appreciate the financial support from Zhejiang Construction Science and Technology Project (1011) and the Open Fund of Key Laboratory in Liaoning Province.

## References

- [1] Marinković S., Radonjanin V., Malešev M., et al., Comparative environmental assessment of natural and recycled aggregate concrete, *Waste Manage.*, 2010,30(11),2255-2264.
- [2] González-Fontbea B., Martínez-Abella F., Concretes with aggregates from demolition waste and silica fume. *Materials and mechanical properties*, *Build. Environ.*, 2008,43(4),429-437.
- [3] Zhang C.B., Hu M.M., Dong L., et al., Eco-efficiency assessment of technological innovations in high-grade concrete recycling, *Resour. Conserv. Recycl.*, 2019,149,649-663.
- [4] Tabsh S.W., Abdelfatah A.S., Influence of recycled concrete aggregates on strength properties of concrete, *Constr. Build. Mater.*, 2009,23(2),1163-1167.
- [5] Zhang N., Zheng L.N., Duan H.B., et al., Differences of methods to quantify construction and demolition waste for less-developed but fast-growing countries: China as a case study, *Environ. Sci. Pollut. Res.*, 2019,26(25),25513-25525.
- [6] Angulo S.C., Ulsen C., John V.M., et al., Chemical-mineralogical characterization of C&DW recycled aggregates from São Paulo, Brazil, *Waste Manage.*, 2009, 29(2),721-730.
- [7] Rao M.C., Bhattacharyya S.K., Barai S.V., Behaviour of recycled aggregate concrete under drop weight impact load, *Constr. Build. Mater.*, 2011,25(1),69-80.
- [8] Poon C.S., Chan D., The use of recycled aggregate in concrete in Hong Kong, *Resour. Conserv. Recycl.*, 2007,50(3),293-305.
- [9] Soutsos M.N., Tang K.K., Millard S.G., Concrete building blocks made with recycled demolition aggregate, *Constr. Build. Mater.*, 2011, 25(2),726-735.
- [10] Evangelista L., de Brito J., Durability performance of concrete made with fine recycled concrete aggregates, *Cem. Concr. Compos.*, 2010,32(1),9-14.
- [11] Zaharieva R., Buyle-Bodin F., Skoczylas F., et al., Assessment of the surface permeation properties of recycled aggregate concrete, *Cem. Concr. Compos.*, 2003,25(2),223-232.
- [12] Sim J., Park C., Compressive strength and resistance to chloride ion penetration and carbonation of recycled aggregate concrete with varying amount of fly ash and fine recycled aggregate, *Waste Manage.*, 2011,31(11),2352-2360.
- [13] Corinaldesi V., Moriconi G., Behaviour of cementitious mortars containing different kinds of recycled aggregate, *Constr. Build. Mater.*, 2009,23(1),289-294.
- [14] Gokce A., Nagataki S., Saeki T., et al., Freezing and thawing resistance of air-entrained concrete incorporating recycled coarse aggregate: The role of air content in demolished concrete, *Cem. Concr. Res.*, 2004,34(5),799-806.
- [15] Zaharieva R., Buyle-Bodin F., Wirquin E., Frost resistance of recycled aggregate concrete, *Cem. Concr. Res.*, 2004,34(10),1927-1932.
- [16] Xiao J.Z., Li J.B., Zhang Ch., Mechanical properties of recycled aggregate concrete under uniaxial loading, *Cem. Concr. Res.*, 2005,35(6),1187-1194.
- [17] Rahal R., Mechanical properties of concrete with recycled coarse aggregate, *Build. Environ.*, 2007,42(1),407-415.
- [18] Lee S.T., Influence of recycled fine aggregates on the resistance of mortars to magnesium sulfate attack, *Waste Manage.*, 2009,29(8),2385-2391.
- [19] Corinaldesi V., Mechanical and elastic behaviour of concretes made of recycled-concrete coarse aggregates, *Constr. Build. Mater.*, 2010,24(9),1616-1620.
- [20] Belén G.F., Fernando M.A., Diego C.L., et al., Stress-strain relationship in axial compression for concrete using recycled saturated coarse aggregate, *Constr. Build. Mater.*, 2011,25(5),2335-2342.
- [21] Butler L., West J.S., Tighe S.L., The effect of recycled concrete aggregate properties on the bond strength between RCA concrete and steel reinforcement, *Cem. Concr. Res.*, 2011,41(10),1037-1049.
- [22] González-Fontbea B., Martínez-Abella F., Shear strength of recycled concrete beams, *Constr. Build. Mater.*, 2007,21(4),887-893.
- [23] Domingo-Cabo A., Lázaro C., López-Gayarre F., et al., Creep and shrinkage of recycled aggregate concrete, *Constr. Build. Mater.*, 2009,23(7),2545-2553.
- [24] Liu Q., Xiao J.Z., Sun Z.H., Experimental study on the failure mechanism of recycled concrete, *Cem. Concr. Res.*, 2011,41(10),1050-1057.
- [25] Fathifazl G., Razaqpur A.G., Isgor O.B., et al., Creep and drying shrinkage characteristics of concrete produced with coarse recycled concrete aggregate, *Cem. Concr. Compos.*, 2011,33(10),1026-1037.
- [26] Tam V.W.Y., Gao X.F., Tam C.M., Microstructural analysis of recycled aggregate concrete produced from two-stage mixing approach, *Cem. Concr. Res.*, 2005,35(6),1195-1203.
- [27] Tam V.W.Y., Tam C.M., Wang Y., Optimization on proportion for recycled aggregate in concrete using two-stage mixing approach, *Constr. Build. Mater.*, 2007,21(10),1928-1939.
- [28] Poon C.S., Shui Z.H., Lam L., et al., Influence of moisture states of natural and recycled aggregates on the slump and compressive strength of concrete, *Cem. Concr. Res.*, 2004,34(1),31-36.
- [29] Kong D.Y., Lei T., Zheng J.J., et al., Effect and mechanism of surface-coating pozzalanics materials around aggregate on properties and ITZ microstructure of recycled aggregate concrete, *Constr. Build. Mater.*, 2010,24(5),701-708.
- [30] Tam V.W.Y., Tam C.M., Diversifying two-stage mixing approach (TSMA) for recycled aggregate concrete: TSMA and TSMAc, *Constr. Build. Mater.*, 2008,22(10),2068-2077.
- [31] Li J.S., Xiao H.N., Zhou Y., Influence of coating recycled aggregate surface with pozzolanic powder on properties of recycled aggregate concrete, *Constr. Build. Mater.*, 2009,23(3),1287-1291.
- [32] Abbas A., Fathifazl G., Isgor O.B., et al., Durability of recycled aggregate concrete designed with equivalent mortar volume method, *Cem. Concr. Compos.*, 2009,31(8),555-563.
- [33] Corinaldesi V., Moriconi G., Influence of mineral additions on the performance of 100% recycled aggregate concrete, *Constr. Build. Mater.*, 2009,23(8),2869-2876.
- [34] Tangchirapat W., Buranasing R., Jaturapitakkul C., et al., Influence of rice husk-bark ash on mechanical properties of concrete containing high amount of recycled aggregates, *Constr. Build. Mater.*, 2008,22(8),1812-1819.
- [35] Mesbah H.A., Buyle-Bodin F., Efficiency of polypropylene and metallic fibres on control of shrinkage and cracking of recycled aggregate mortars, *Constr. Build. Mater.*, 1999,13(8),439-447.
- [36] Akbarnezhad A., Ong K.C.G., Zhang M.H., et al., Microwave-assisted beneficiation of recycled concrete aggregates, *Constr. Build. Mater.*, 2011,25(8),3469-3479.
- [37] Shui Z.H., Xuan D.X., Wan H.W., et al., Rehydration reactivity of recycled mortar from concrete waste experienced to thermal treatment, *Constr. Build. Mater.*, 2008,22(8),1723-1729.



- [38] Etxeberria M., Vázquez E., Marí A., et al., Influence of amount of recycled coarse aggregates and production process on properties of recycled aggregate concrete, *Cem. Concr. Res.*, 2007, 37(5), 735-742.
- [39] Poon C.S., Shui Z.H., Lam L., Effect of microstructure of ITZ on compressive strength of concrete prepared with recycled aggregates, *Constr. Build. Mater.*, 2004, 18(6), 461-468.
- [40] Xiao J.Z., Li W.G., Corr D.J., et al., Effects of interfacial transition zones on the stress-strain behavior of modeled recycled aggregate concrete, *Cem. Concr. Res.*, 2013, 52, 82-99.
- [41] Tao J., Preliminary study on the water permeability and microstructure of concrete incorporating nano-SiO<sub>2</sub>, *Cem. Concr. Res.*, 2005, 35(10), 1943-1947.
- [42] Li H., Zhang M.H., Ou J.P., Flexural fatigue performance of concrete containing nano-particles for pavement, *Int. J. Fatigue*, 2007, 29(7), 1292-1301.
- [43] Zhang M.H., Li H., Pore structure and chloride permeability of concrete containing nano-particles for pavement, *Constr. Build. Mater.*, 2011, 25(2), 608-616.
- [44] Nazari A., Riahi S., The effect of TiO<sub>2</sub> nanoparticles on water permeability and thermal and mechanical properties of high strength self-compacting concrete, *Mater. Sci. Eng. A-Struct. Mater. Prop.*, 2010, 528(2), 756-763.
- [45] Nazari A., Riahi S., The effects of SiO<sub>2</sub> nanoparticles on physical and mechanical properties of high strength compacting concrete, *Compos. Pt. B-Eng.*, 2011, 42(3), 570-578.
- [46] Nazari A., Riahi S., Microstructural, thermal, physical and mechanical behavior of the self-compacting concrete containing SiO<sub>2</sub> nanoparticles, *Mater. Sci. Eng. A-Struct. Mater. Prop.*, 2010, 527(29-30), 7663-7672.
- [47] Zhang H.R., Zhao Y.X., Meng T., et al., Surface Treatment on Recycled Coarse Aggregates with Nanomaterials, *J. Mater. Civ. Eng.*, 2016, 28(2), 04015094-1-04015094-11.
- [48] Zhang H.R., Zhao Y.X., Meng T., et al., The modification effects of a nano-silica slurry on microstructure, strength, and strain development of recycled aggregate concrete applied in an enlarged structural test, *Constr. Build. Mater.*, 2015, 95, 721-735.
- [49] Tam V.W.Y., Gao X.F., Tam C.M., et al., New approach in measuring water absorption of recycled aggregates, *Constr. Build. Mater.*, 2008, 22(3), 364-369.
- [50] Scrivener K.L., Nemat K.M., The percolation of pore space in the cement paste aggregate interfacial zone of concrete, *Cem. Concr. Res.*, 1996, 26(1), 35-40.
- [51] Zheng J.J., Wong H.S., Buenfeld N.R., Assessing the influence of ITZ on the steady-state chloride diffusivity of concrete using a numerical model, *Cem. Concr. Res.*, 2009, 39(9), 805-813.
- [52] Akçaoğlu T., Tokyay M., Çelik T., Effect of coarse aggregate size and matrix quality on ITZ and failure behavior of concrete under uniaxial compression, *Cem. Concr. Compos.*, 2004, 26(6), 633-638.
- [53] Ke Y., Ortola S., Beaucour A.L., et al., Identification of microstructural characteristics in lightweight aggregate concretes by micromechanical modelling including the interfacial transition zone (ITZ), *Cem. Concr. Res.*, 2010, 40(11), 1590-1600.
- [54] Belaïd F., Arliguie G., François R., Porous structure of the ITZ around galvanized and ordinary steel reinforcements, *Cem. Concr. Res.*, 2001, 31(11), 1561-1566.
- [55] Diamond S., Considerations in image analysis as applied to investigations of ITZ in concrete, *Cem. Concr. Compos.*, 2001, 23(2-3), 171-178.